UCRL-JC-127993
PREPRINT

Burn Rates of Pristine and Degraded Explosives At Elevated Temperatures and Pressures

Jon L. Maienschein
Jeffrey B. Chandler

This paper was prepared for submittal to the
Eleventh International Detonation (1998) Symposium
Snowmass, CO
Aug. 31- Sept. 4, 1998

August 10, 1998

Lawrence
Livermore
National
Laboratory

BURN RATES OF PRISTINE AND DEGRADED EXPLOSIVES AT ELEVATED TEMPERATURES AND PRESSURES

Jon L. Maienschein, Jeffrey B. Chandler
Lawrence Livermore National Laboratory
P.O. Box 808, L-282
Livermore, CA 94550

We measure the laminar burn rates of explosives at extreme conditions (up to 520K and 1 GPa) in a hybrid strand burner, to provide reaction rate data for prediction of violence of thermal response. Data from a series of HMX-based explosives show that explosives with high binder content (15 wt%) burn smoothly over the entire pressure range regardless of particle size, while explosives with less binder eventually transition to a rapid erratic burn 10-100 times faster. When heated to ≈ 440K, an HMX formulation with fine particles and 15% binder exhibits different burning behavior depending on the details of the temperature-pressure history, apparently as a result of the $\beta \rightarrow \delta$ phase transition in HMX. Burn rates can be increased by 1000-fold under certain conditions.

INTRODUCTION

In considering hazards from explosives, thermal response of explosives exposed to high temperatures, as in a fire, is of general interest. Understanding and prediction of the violence of thermally-driven reactions (i.e., slow and fast cookoff) is the focus of several current research efforts. The violence of a thermal reaction is affected by the balance between heat release by exothermic combustion reactions and heat dissipation by thermal diffusion. The topic of this paper is quantification of the first process by measurement of the burn rate of pristine and thermally-degraded explosives at high temperatures and pressures. We approach as closely as possible the conditions that exist during cookoff of energetic materials, with pressure of thousands of atmospheres and temperatures of several hundred degrees Celsius. Here we report measurements on several HMX – based formulations under different conditions of temperature and pressure. In addition, we are assessing the effect of thermal damage on violence by measuring burn rates at different levels of thermal decomposition.

EXPERIMENTAL APPARATUS

The hybrid strand burner/closed bomb system, shown in Figure 1, combines the features of a traditional closed-bomb burner with those of a traditional strand burner. In a standard closed-bomb burner, pressure in the combustion chamber is the only measurement, with no measure of the surface regression rate to check combustion uniformity. With this design the data from samples that burn erratically are particularly hard to interpret. The standard strand burner provides direct measurement of the surface regression rate in a large volume at constant pressure, giving only one data point of rate *vs* pressure in each experiment; further, the large volume required for isobaric operation means that operation at high pressures is generally not practical. In contrast, our hybrid strand burner/closed bomb system burns a sample in a small constant-volume (≈ 70 cm^3), high-pressure (up to 400 MPa initial, > 1 GPa final) chamber; temporal pressure data and burn front time-of-arrival data provide surface regression and mass regression data for a range of pressures in one experiment.

The burn sample, 64 mm long and 6.4 mm in diameter, is generally formed by stacking nine pellets end-to-end, with 75 μm diameter silver burn wires between

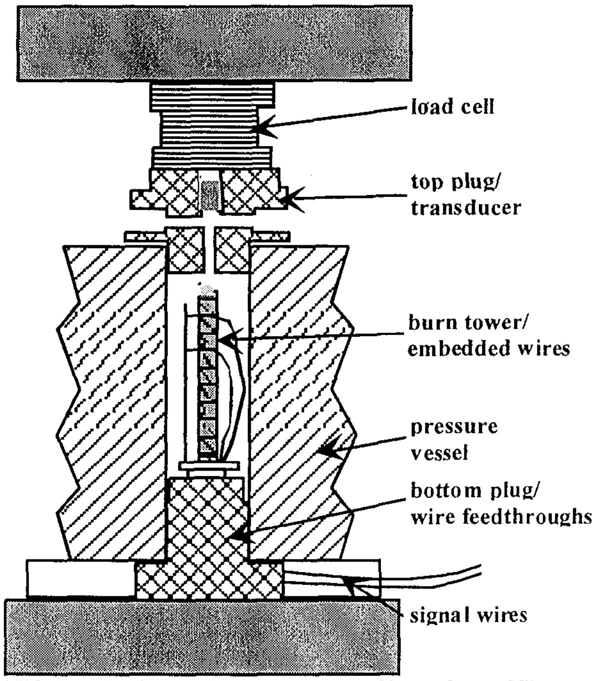

FIGURE 1. SCHEMATIC OF HYBRID STRAND BURNER.

each pair of pellets and at top and bottom. The stack is coated with an epoxy (Epon 82 with Versamid 140 catalyst) on its cylindrical surface to restrict combustion to the end of the sample. The ignition system at the sample top is a hot wire embedded in boron potassium nitrate, which then lights a thin HNS pellet.

The strand burner is prepressurized, generally with argon, to the desired starting pressure before igniting the burn; this initial pressure can range from 5-400 MPa. During the burn we use a load cell and/or a pressure transducer to measure the temporal pressure in the bomb; because of the small bomb volume, the pressure increases 3-6 fold during a burn. We detect the arrival of the burn front by the burning through of wires embedded in the sample. A high speed digitizer captures the data for subsequent analysis. Burn wires are recorded in a way that we can unambiguously assign each signal to a particular wire; occasionally a wire will report out of sequence if it is broken by debris in the bomb chamber. Typical data are shown in Figure 2, along with the pressure signal. Faster-burning segments can be seen in both the pressure and wire data, providing confirmation that the apparent non-uniform burning rate is real and not an artifact of the experiment.

The burn wire electronics provide a well-defined signal, with rise time less than 40 microseconds. The wires burn through reproducibly, with wires mounted at the same location in the sample showing a standard deviation of about 2 milliseconds. The wires do take several milliseconds to burn through; however, this time is essentially independent of initial pressure and temperature conditions and therefore does not affect the burn rate calculation made by differences in times-of-arrival. The burn wire at the bottom of the stack does not burn through unless enough energetic material is placed below it to provide several milliseconds of burning once the flame front has passed.

We calculate burn rate using the location-time data from the wires. We calculate the burn rate from the elapsed time to burn each pair of pellets, and the associated average pressure, to smooth the data somewhat. We do not calculate the burn rate from the pressure-time record, thereby avoiding the uncertainties in the equation of state of the combustion products and heat loss to the vessel walls (this is particularly important for prepressurized experiments, since the equation of state of argon at 200-400 MPa is not modeled well in conventional thermochemical packages.[1] We do use the pressure data to confirm observations from the wire data.

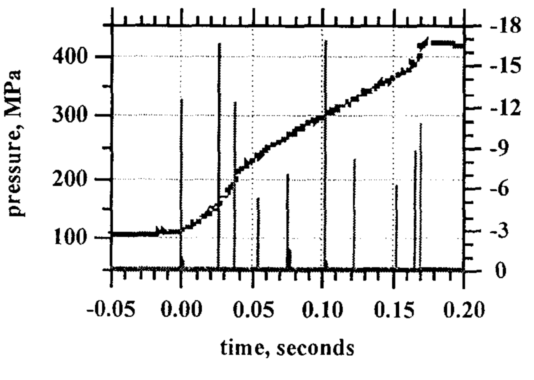

FIGURE 2. TYPICAL PRESSURE AND WIRE DATA FROM THE STRAND BURNER

RESULTS AND DISCUSSION

BASELINE DATA – LX-04

Our baseline explosive, LX-04, contains 85 wt% HMX and 15 wt% Viton-A, with fine particle "LX-04 grade" HMX (no particles ≥ 300 μm, 90% ≤ 100 μm, and 35-50% < 44 μm). Pellets were uniaxially pressed to 98-99% of TMD. The combination of fine particle size and high binder content results in a smoothly-burning formulation over all pressure conditions at ambient temperature. Burn rate data for LX-04 at 300K initial temperature are shown in Figure 3. Two sets of data are included, with pressure measured either by load cell or by pressure transducer. The pressure error bars indicate that the load cell is less precise than the pressure transducer, so when possible the load cell is not used; currently we are limited to the load cell for runs at elevated temperature or with materials with corrosive products. For LX-04, both sets of data are consistent and give a burn rate linear in pressure over the pressure range 10-500 MPa. The burn rate error bars show that the error is larger at fast burn rates; there is an inherent noise of ≈ 1-2 millisecond in the wire time to burn, and at the faster burn rates this becomes a significant contribution to the error.

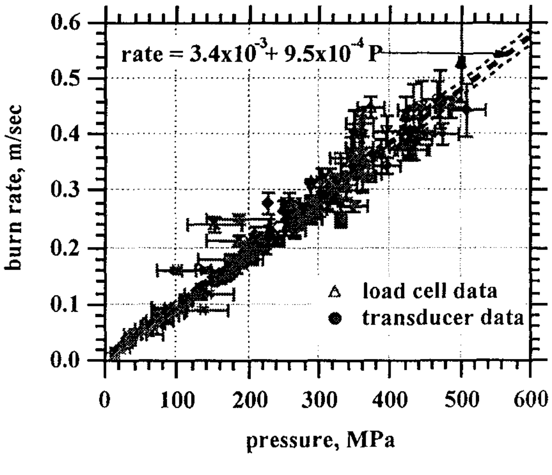

FIGURE 3. LX-04 BURN RATE DATA AT 300K (85 WT% HMX, 15 WT% VITON-A).

In Figure 3 we show a linear fit of burn rate to pressure with the error envelope as dashed lines. If we allowed the pressure exponent to vary, the best value was 0.95, not significantly different from 1.0, so we chose to use the linear description. The data in Figure 3 are compared with literature data[2-4] for pure HMX (crystals and pressed powder) burn rate in Figure 4. We see that the LX-04 burns somewhat slower, as would be expected with its 15% inert binder. However, the overall agreement demonstrates the validity of this measurement technique.

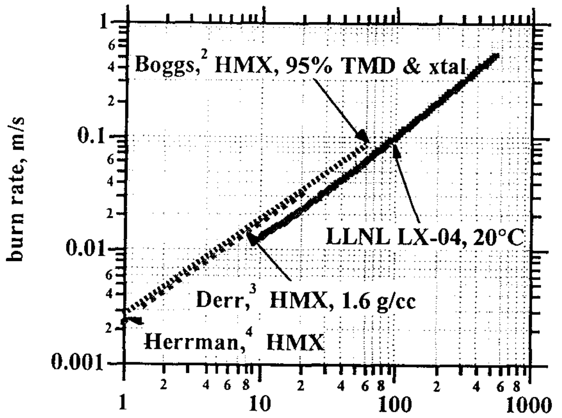

FIGURE 4. COMPARISON OF LX-04 RESULTS WITH LITERATURE HMX DATA.

EFFECT OF BINDER CONTENT AND PARTICLE SIZE

Variations in formulations allowed us to determine the effect of binder content and particle size on burn behavior. The formulation LX-07 contains 90 wt% HMX and 10 wt% Viton-A, with fine-particle "LX-04 grade" HMX. Its burn behavior, shown in Figure 5, is the same as LX-04 at low pressure but very rapid and erratic at high pressures (> 100 MPa). This deconsolidative burning has been reported in the literature,[2,5,6] and is apparently the result of physical failure of the sample at high pressure leading to increased surface area and faster burn rate. Deconsolidative burning is seen at lower pressures with binderless HMX pressed powder samples;[2,5] it is reasonable to expect it at higher pressures for plastic-bonded explosives that are more physically robust.

The effect of particle size was determined using formulation RX-04-AN, with 85 wt% HMX and 15 wt% Viton-A; this has the same composition as LX-04, but contains larger-particle "LX-10 grade" HMX (≈ 6% > 300 μm, ≈ 30% 125-300 μm, ≈ 40% 44-125 μm, and ≈ 24% < 44 μm). As shown in Figure 6, this formulation burns smoothly over the entire pressure range with no deconsolidative behavior. The burn rate of RX-04-AN was lower than that of LX-04. This is consistent with the particle size difference – we would expect that larger-particle material would burn more slowly with its reduced HMX surface area per unit volume of explosive.

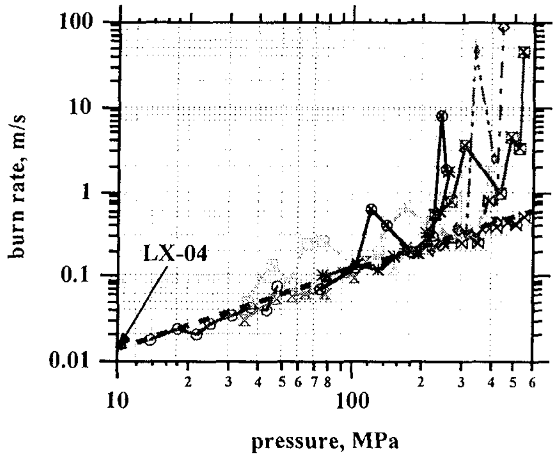

FIGURE 5. LX-07 BURN RATE DATA (90 WT% HMX, 10 WT% VITON-A, FINE PARTICLE HMX).

The data in Figures 5 and 6 allow us to conclude that, at least for formulations containing HMX and Viton-A, a low binder content (≤ 10 wt%) will lead to erratic deconsolidative burning with rates increased up to 100-fold. However, the presence of large-particle HMX alone does not lead to deconsolidative burning. One possible cause of deconsolidative burning, the fracture of large HMX particles with increasing pressure leading to increased surface area, does not seem to be operative in RX-04-AN.

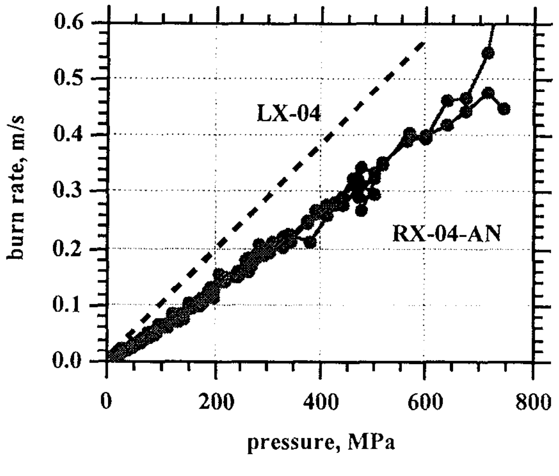

FIGURE 6. RX-04-AN BURN RATE (85 WT% HMX, 15 WT% VITON-A, COARSE PARTICLE HMX).

We also made burn rate measurements on two HMX formulations with large particles and ≈ 5 wt% binder. LX-10-1 is 94.5 wt% HMX and 5.5 wt% Viton-A, with the same particle size distribution as RX-04-AN. PBX-9501 is 95 wt% HMX, 2.5 wt% Estane, and 2.5 wt% BDNPA/F, with a similar particle size distribution (8% > 300 μm, ≈ 37% 125-300 μm, ≈ 30% 44-125 μm, and ≈ 25% < 44 μm) Burn rate data for these formulations are shown in Figures 7 and 8. Both formulations show the onset of deconsolidative burning at ≈ 150 MPa, with the burn rates increasing almost 1000-fold.

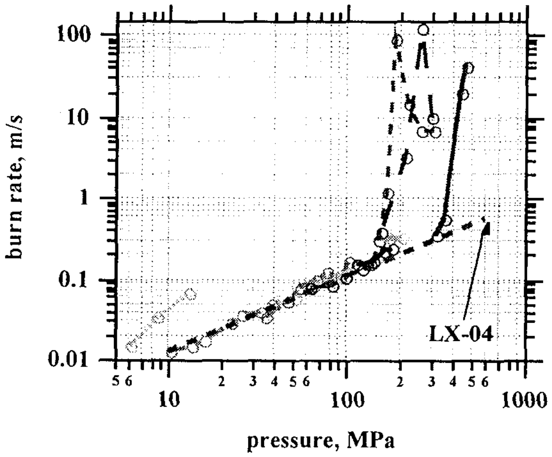

FIGURE 7. LX-10 BURN RATE (94.5 WT% HMX, 5.5 WT% VITON-A, COARSE PARTICLE HMX).

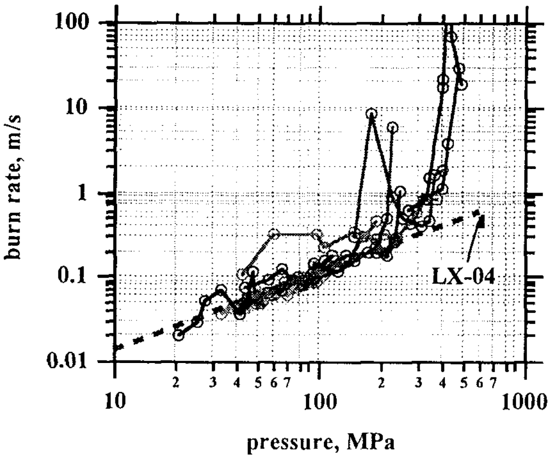

FIGURE 8. PBX-9501 BURN RATE (95 WT% HMX, 2.5 WT% ESTANE, 2.5 WT% BDNPA/F, COARSE PARTICLE HMX).

At pressures below the onset of deconsolidation, the LX-10 and PBX-9501 burn rates are essentially the same as that of LX-04, in contrast to the slower rate of RX-04-AN with a similar particle size distribution. One plausible explanation is that the reduction in burn rate by larger particles is offset by an increase in burn rate with reduced binder content and hence increased combustion energy. We did not observe such an effect in comparing 15 wt% and 10 wt% binder (LX-04 and LX-07), but the relative increase in combustion energy is much higher for the 5 wt% binder formulations.

BURN BEHAVIOR AT HIGH TEMPERATURE

To measure burn rate at high temperature, we heat the pressure vessel to ≈ 400K with external band heaters, and bring the sample to the final higher temperature with an internal heating element. For some measurements we held the samples at elevated temperatures for a prolonged period before pressurizing and burning.

We measured the burn rate of LX-04 at two temperature ranges: 418-428K and 438-453K. These are below and above the transition temperature for the $\beta \rightarrow \delta$ solid-solid phase transition of ≈ 433K,[7-11] inasmuch as we expected the phase transition to affect the burn behavior. To obtain the data shown in Figure 9, the strand burner was pressurized to the starting pressure before the heaters were turn on. The samples were heated and held at temperature for about 10 minutes before burning. Based on Behrens' thermal decomposition data for HMX,[12-14] we expect insignificant thermal degradation during this period; therefore we are measuring the effect of burn rate on undegraded hot HMX.

In Figure 9 we see that the burn rates for LX-04 at pressures > 100 MPa are only slightly (≈ 20%) faster for the heated samples than for samples at 300K; furthermore there is no significant difference between the lower

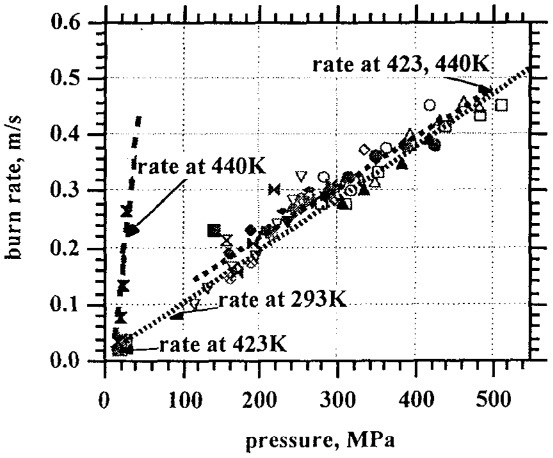

FIGURE 9. BURN BEHAVIOR OF LX-04 AT ELEVATED TEMPERATURE. HOLLOW SYMBOLS ARE FOR RUNS AT 418-438K, SOLID SYMOBLS FOR 438-453K.

and higher temperature runs. However, at lower pressures the temperature plays a key role. The burn rate at 423K is essentially unchanged from that at 300K, while the burn rate at 440K is greatly accelerated. This can be explained by the pressure dependence of the $\beta \rightarrow \delta$ solid-solid phase transition. This phase transition is kinetically limited, and is retarded by high pressure because of the accompanying decrease in density.[15-17] At 100 MPa the phase transition temperature increases to about 480-490K.[15] Therefore, in the runs that were pressurized to this extent before heating, the phase transition was suppressed and the burn rate is that of β-phase. However, for the runs with initial pressure of 15 MPa, the phase conversion presumably took place to some unknown extent during heating, and the burn rate is that of a mixed β-phase and δ-phase HMX in LX-04.

The phase change may impact the burn behavior in a couple of ways. The phase change results in a density decrease of about 8%,[7] which will cause physical disruption of the sample and production of defects through which combustion gases can propagate. In addition, the δ-phase of HMX is more sensitive to mechanical impact than β-phase HMX, and the δ-phase may inherently have a faster burning rate as well. These effects may be sorted out in future experiments where δ-phase HMX is tested directly.

To study the effect of thermal degradation, we heated LX-04 for 22 hours at different temperatures, and then measured the burn rate. From Behren's HMX decomposition data, [12-14] we expect the degree of decomposition to be low, but we expect some decomposition at ≈ 450K. Because of the design of the equipment, we could not hold the sample under pressure during the prolonged heating period, so for these runs the LX-04 was heated while at atmospheric pressure. The results are shown in Figure 10, along with fits to the data in Figure 9 for heating without holding, for comparison. Three runs were made with a 22-hour soak at 453K, above the $\beta \rightarrow \delta$ phase transition temperature. The measured burn rates were very high for these. To confirm the effect of the phase transition, three runs were made at 423K, below the phase transition temperature. These, however, gave rather scattered results, with one run showing almost the same burn rate as the higher-temperature runs, one showing intermediate values, and one showing a burn rate barely above that of the prepressurized and undegraded LX-04. It therefore appears that other processes in addition to the $\beta \rightarrow \delta$ phase transition are occurring in the heated LX-04. We plan further experimental work to clarify this behavior.

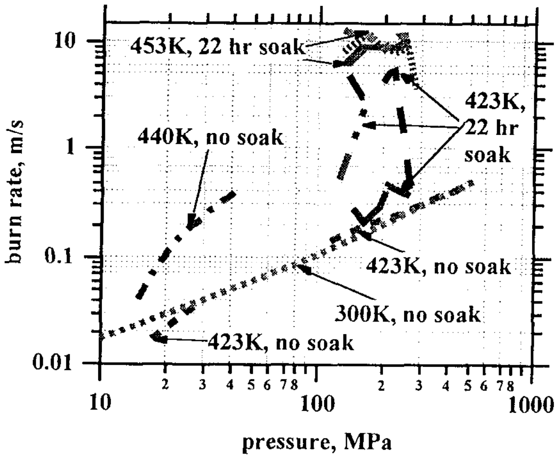

FIGURE 10. BURN BEHAVIOR FOR LX-04 HEATED AND HELD AT TEMPERATURE FOR 22 HOURS. SAMPLES HEATED WITH NO SOAK WERE PRESSURIZED PRIOR TO HEATING. SAMPLES HEATED WITH SOAK WERE PRESSURIZED AFTER THERMAL TREATMENT.

IMPLICATIONS OF OBSERVED BURN BEHAVIOR FOR THERMAL RESPONSE

We have quantified the burn rate at ambient temperature fairly well for several formulations with Viton A binder and estane binders. More importantly, we have identified conditions (e.g. low binder content and heating > 430K at low pressure) that lead to a 10-1000 fold increase in burn rate. Low binder content presumably results in physical failure of the sample with a concomitant increase in surface area and burn rate. Heating > 430K at low pressure causes the $\beta \rightarrow \delta$ phase transition, which physically disrupts the sample with the 8% density decrease; the combustion gases apparently propagate through the defects and again result in a very fast burn. Both of these mechanisms are physical in nature, not chemical, but both will certainly play a significant role in the overall violence of a thermal reaction.

To predict the violence of a thermal reaction, the burn rate of the explosive must be accurately understood and described. The data reported here indicate areas where further work is needed, but do not represent thorough understanding of the phenomena involved. In particular, the behavior of heated explosives requires further study before we can quantify it sufficiently to allow meaningful prediction of violence.

We can draw one conclusion from this work. The violence of thermal response of HMX-based formulations will be strongly affected by the binder content; formulations with 5 –10 wt% binder are expected to give much more violent explosions than those containing higher levels of binder.

These data will allow development of burn rate models to be used in simulation computer codes being constructed at LLNL and elsewhere to predict the violence of thermal response. All effects must be included in the codes for realistic simulations. Because of the importance of the HMX phase transition, computer codes must be able to treat solid-solid phase transitions, and must follow the time-temperature-pressure history to have the information necessary to know the phase state of the HMX.

FUTURE WORK

The effects that lead to greatly-changed burn behavior must be well-characterized in order to be accurately included in response models. Future work will be focused accordingly. Of particular importance is quantification of the effect of preheating on burn behavior; the erratic behavior seen in Figure 10 for thermal degradation at 423K is of special interest. We are undertaking thermal soak experiments at elevated pressures, to remove the effect of phase change. Also of interest is the study of δ-phase HMX to determine if the phase change effect is merely physical disruption of the sample or if δ-phase is inherently faster burning. Other measurements will be undertaken as appropriate to address the issue of thermal reaction violence.

CONCLUSIONS

The burn rate of HMX-based explosives has been characterized by measurement in a high pressure hybrid strand burner. Through measurements on robust HMX-Viton-A formulations, we have established an inherent burn rate of HMX formulations, subject to minor variations driven by formulation details. We have also identified conditions of formulation details and burn environment that lead to erratic and greatly-accelerated burn rates. This rapid erratic burn behavior may well dominate the determination of violence of thermal response of explosives, and will be the subject of further study.

ACKNOWLEDGEMENTS

Support for this work was provided by the LLNL Energetic Materials Surety Program and by the DoD/DOE Memorandum of Understanding.

We thank Jack Reaugh for insightful comments on the operation and interpretation of strand burner data, Dan Greenwood for expertise in providing robust and accurate electronic diagnostic systems, Jeff Wardell for converting the laborious sample assembly procedure into a streamlined mass-production methodology, Rich Simpson for tireless pressing of the hundreds of pellets consumed in the work, Lonnis Daniels for assembly of many burn samples, and Don Hansen for mechanical support.

This work was performed under the auspices of the U.S. Department of Energy by the Lawrence Livermore National Laboratory under contract number W-7405-Eng-48.

REFERENCES

1. Fried, L.E., "CHEETAH 1.39 User's Manual", Lawrence Livermore National Laboratory, UCRL-MA-117541 Rev. 3 (March 19, 1996).

2. Boggs, T.L., "Thermal Behavior of Cyclotrimethylenetrinitramine(RDX) and Cyclotetramethylenetetranitramine (HMX) ", in Kuo, K.S. and Summerfield, M., **Fundamentals of Solid-Propellant Combustion**, vol. 90, American Institute of Aeronautics and Astronautics, New York (1984).

3. Derr, R.L., Boggs, T.L., Zurn, D.E. and Dibble, E.J., "The Combustion Characteristics of HMX", in **Proceedings of 11th JANNAF Combustion Meeting,** Pasadena, CA, CPIA, p. 231 (1974).

4. Herrmann, M., Engel, W. and Eisenreich, N., "Thermal Expansion, Transitions, Sensitivities and Burning Rates of HMX", *Propellants, Explosives, Pyrotechnics*, **17**, 190 (1992).

5. Fifer, R.A. and Cole, J.E., "Transitions from Laminar Burning for Porous Crystalline Explosives", in **Proceedings of the Seventh Symposium (International) of Detonation**, Annapolis, MD, Office of Naval Research, NSWC MP-82-334, p. 164 (1981).

6. Tao, W.C., Costantino, M.S. and Ornellas, D.L., "Burning Rates of Two Cast Nitramine Explosives Using a Hybrid Closed Bomb-Strand Burner", in **Proceedings of the Ninth Symposium (International) of Detonation**, Portland, OR, Office of the Chief of Naval Research, OCNR 113291-7, p. 1310 (1989).

7. Cady, H.H., "Studies on the Polymorphs of HMX", Los Alamos Scientific Laboratory, LAMS-2652 (October 18, 1961).

8. Cobbledick, R.E. and Small, R.W.H., "The Crystal Structure of the δ-form of 1, 3, 5, 6 - Tetranitro-1, 3, 5, 7-tetraazacyclooctane (δ-HMX) ", *Acta Cryst.*, **B30**, 1918 (1974).

9. Teetsov, A.S. and McCrone, W.C., "The Microscopial Study of Polymorph Stability Diagrams", *Microscop. Cryst. Front.*, **15**, 13 (1965).

10. McCrone, W.C., "Crystallographic Data: Cyclotetramethylene Tetranitramine (HMX) ", *Analytical Chem.*, **22**, 1225 (1950).

11. Herrmann, M., Engel, W. and Eisenreich, N., "Phase Transitions of HMX and their Significance for the Sensitivity of Explosives", in **Proceedings of the Technical Meeting of Specialists MWDDEA AF-71-F/G-7304 - Physics of Explosives**, Saint-Louis, 26.6.1990 p. 12 (1990).

12. Behrens, R., "Thermal decomposition of energetic materials: temporal behaviors of the rates of formation of the gaseous products from condensed-phase decomposition of octahydro-1,3,5,7-tetranitro-1,3,5,7-tetrazocine", *J. Phys. Chem.*, **94**, 6706 (1990).

13. Behrens, R., "Thermal decomposition of HMX and RDX: decomposition processes and mechanisms based on STMBMS and TOF velocity-spectra measurements", in Bulusu, S.N., **Chemistry and Physics of Energetic Materials**, Kluwer Academic Publishers, the Netherlands (1990).

14. Behrens, R., "Identification of octahydro-1,3,5,6-tetranitro-1,3,5,7-tetrazocine (HMX) pyrolysis products by simultaneous thermogravimetric modulated beam mass spectrometry and time-of-flight velocity-spectra measurements", *Int. J. Chem. Kin.*, **22**, 135 (1990).

15. Karpowicz, R.J. and Brill, T.B., "The β—δ Transformation of HMX: Its Thermal Analysis and Relationship to Propellants", *AIAA Journal*, **20**, **1586** (1982).

16. Landers, A.G. and Brill, T.B., "Pressure-Temperature Dependence of the β—δ Polymorph Interconversion in Octahydro-1,3,5,7-tetranitro-1,3,5,7-tetrazocine", *J. Phys. Chem*, **84**, 3573 (1980).

17. Karpowicz, R.J., Gelfand, L.S. and Brill, T.B., "Application of Solid-Phase Transition Kinetics to the Properties of HMX", *AIAA Journal*, (1982?).